Cell Reports
Medicine

Article

Neoadjuvant immunotherapy, chemotherapy, and combination therapy in muscle-invasive bladder cancer: A multi-center real-world retrospective study

Graphical abstract

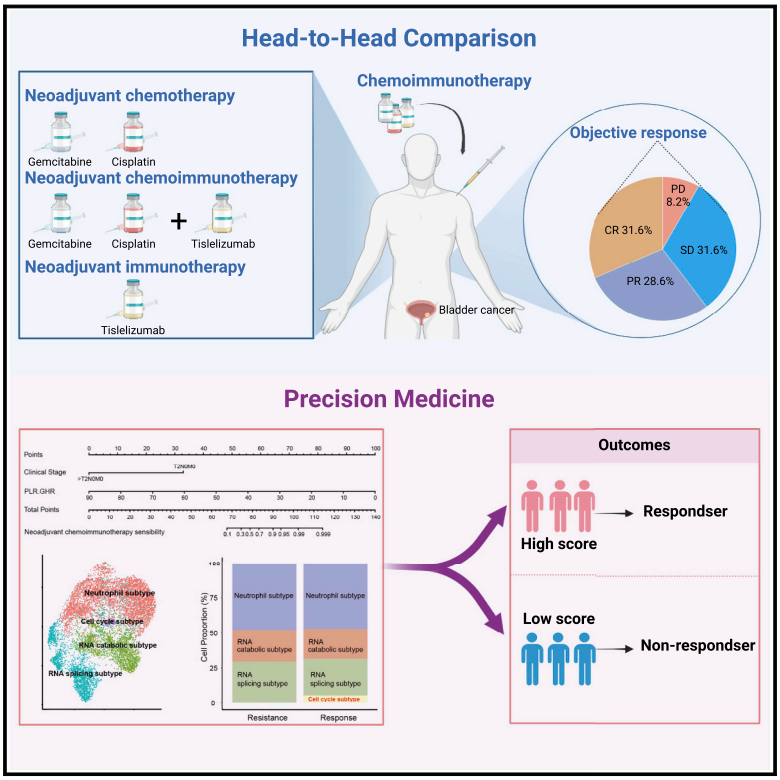

Highlights

- Neoadjuvant chemoimmunotherapy is safe and feasible for patients with bladder cancer
- An efficacy prediction model for neoadjuvant chemoimmunotherapy is developed
- Efficacy biomarkers are explored from bulk and single-cell RNA sequencing

Authors

Jiao Hu, Jinbo Chen, Zhenyu Ou, ..., Chunyu Zhang, Zhi Liu, Xiongbing Zu

Correspondence

zuxbxy@csu.edu.cn

In brief

In a multi-center, real-world study, Hu et al. demonstrate that neoadjuvant chemoimmunotherapy achieves the highest response rate, compared with neoadjuvant immunotherapy or chemotherapy. Patients who achieve pathological complete response after neoadjuvant treatments plus maximal transurethral resection of the bladder tumor may be safe to receive bladder preservation therapy.

Hu et al., 2022, Cell Reports Medicine 3, 100785
November 15, 2022 © 2022 The Author(s).
https://doi.org/10.1016/j.xcrm.2022.100785

CellPress

Cell Reports Medicine

CellPress
OPEN ACCESS

Article

Neoadjuvant immunotherapy, chemotherapy, and combination therapy in muscle-invasive bladder cancer: A multi-center real-world retrospective study

Jiao Hu,[1,2] Jinbo Chen,[1,2] Zhenyu Ou,[1,2] Haige Chen,[3] Zheng Liu,[4] Minfeng Chen,[1,2] Ruiyun Zhang,[3] Anze Yu,[5] Rui Cao,[6] Enchong Zhang,[7] Xi Guo,[8] Bo Peng,[9] Dingshan Deng,[1,2] Chunliang Cheng,[1,2] Jinhui Liu,[1,2] Huihuang Li,[1,2] Yihua Zou,[10] Ruoping Deng,[11] Gang Qin,[11] Wenze Li,[12] Lue Wang,[13] Tao Chen,[14] Xiaming Pei,[15] Guanghui Gong,[16] Jiansheng Tang,[17] Belaydi Othmane,[1,2] Zhiyong Cai,[1,2] Chunyu Zhang,[1,2] Zhi Liu,[1,2] and Xiongbing Zu[1,2,18,*]

[1]Department of Urology, Xiangya Hospital, Central South University, Changsha, China
[2]National Clinical Research Center for Geriatric Disorders, Xiangya Hospital, Central South University, Changsha, China
[3]Department of Urology, Renji Hospital, School of Medicine, Shanghai Jiao Tong University, Shanghai, China
[4]Department of Urology, Tongji Hospital, Huazhong University of Science & Technology, Wuhan, China
[5]Department of Urology, the First Affiliated Hospital, Sun Yat-sen University, Guangzhou, China
[6]Department of Urology, Beijing Friendship Hospital, Capital Medical University, Beijing, China
[7]Department of Urology, Shengjing Hospital, China Medical University, Shenyang, China
[8]Department of Urology, Hunan Provincial People's Hospital, the First Affiliated Hospital of Hunan Normal University, Changsha, China
[9]Department of Urology, Zhangjiajie People's Hospital, Zhangjiajie, China
[10]Department of Urology, the First People's Hospital of Chenzhou, Chenzhou, China
[11]Department of Urology, the Central Hospital of Yongzhou, Yongzhou, China
[12]Department of Urology, the First People's Hospital of Xiangtan City, Xiangtan, China
[13]Department of Urology, Huarong People's Hospital, Yueyang, China
[14]Department of Urology, Xiangyang Central Hospital, Xiangyang, China
[15]Department of Urology, Hunan Cancer Hospital, Changsha, China
[16]Department of Pathology, Xiangya Hospital, Central South University, Changsha, China
[17]Department of Urology, the Affiliated Hospital of Xiangnan University, Xiangnan University, Chenzhou, China
[18]Lead contact
*Correspondence: zuxbxy@csu.edu.cn
https://doi.org/10.1016/j.xcrm.2022.100785

SUMMARY

To parallelly compare the efficacy of neoadjuvant immunotherapy (tislelizumab), neoadjuvant chemotherapy (gemcitabine and cisplatin), and neoadjuvant combination therapy (tislelizumab + GC) in patients with muscle-invasive bladder cancer (MIBC) and explore the efficacy predictors, we perform a multi-center, real-world cohort study that enrolls 253 patients treated with neoadjuvant treatments (combination therapy: 98, chemotherapy: 107, and immunotherapy: 48) from 15 tertiary hospitals. We demonstrate that neoadjuvant combination therapy achieves the highest complete response rate and pathological downstaging rate compared with neoadjuvant immunotherapy or chemotherapy. We develop and validate an efficacy prediction model consisting of pretreatment clinical characteristics, which can pinpoint candidates to receive neoadjuvant combination therapy. We also preliminarily reveal that patients who achieve pathological complete response after neoadjuvant treatments plus maximal transurethral resection of the bladder tumor may be safe to receive bladder preservation therapy. Overall, this study highlights the benefit of neoadjuvant combination therapy based on tislelizumab for MIBC.

INTRODUCTION

Neoadjuvant chemotherapy (NAC) followed by radical cystectomy (RC) is the standard treatment for muscle-invasive bladder cancer (MIBC). Despite receiving aggressive treatments (NAC + RC), more than 40% of MIBC patients still underwent recurrence or death within 3 years.[1–3] Moreover, NAC remains underutilized in most patients because of cisplatin-ineligible or chemotherapy-related toxicity.[4,5] There is an urgent need for developing new treatment options for patients with MIBC. Recently, immune checkpoint blockade (ICB), including anti-PD-1/PD-L1, showed promising survival benefits and revolutionized the treatment status for patients with advanced MIBC.[6,7] The safety and efficacy of neoadjuvant ICB (NICB) in MIBC has been confirmed by two prospective clinical trials, including PURE-01 and ABACUS studies.[8,9] Similarly, Rose et al. recently reported the safety and efficacy of the combination therapy (NAC.NICB) of NAC and NICB in MIBC.[10] These clinical trials preliminarily laid the

This is an open access article under the CC BY-NC-ND license (http://creativecommons.org/licenses/by-nc-nd/4.0/).

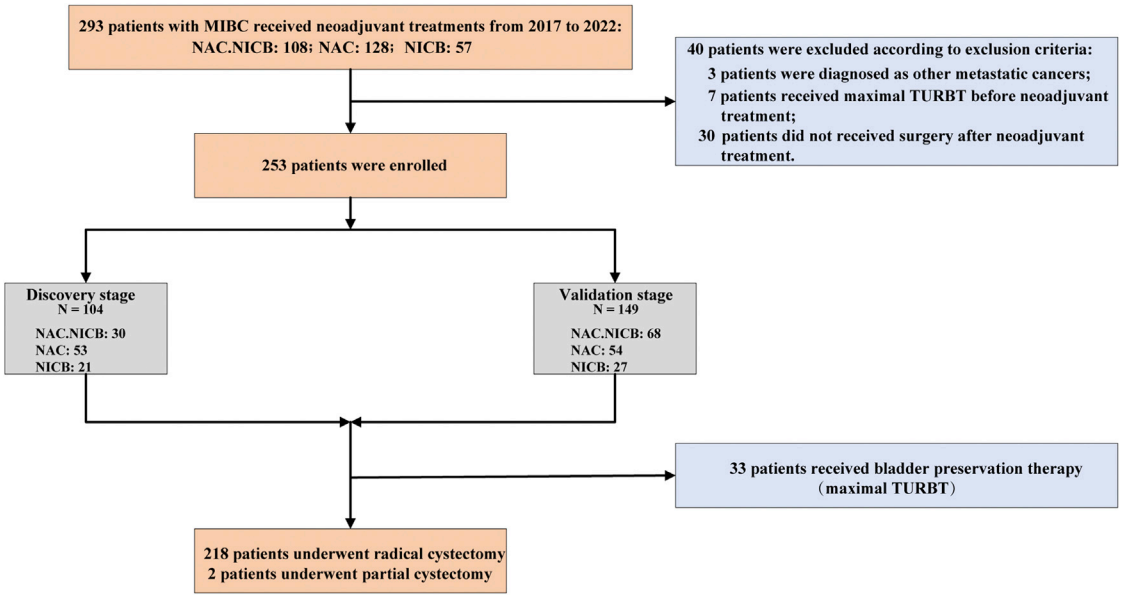

Figure 1. The flow diagram of patient selection

NAC.NICB: combination of neoadjuvant chemotherapy and immunotherapy; NAC: neoadjuvant chemotherapy; NICB: neoadjuvant immunotherapy; TURBT: transurethral resection of the bladder tumor.

foundation for the clinical application of neoadjuvant treatments based on anti-PD-1/PD-L1 in MIBC.

However, several major issues need to be further explored for the neoadjuvant settings of anti-PD-1/PD-L1 in MIBC. First, the tumor control efficacy of NAC, NICB, or NAC.NICB seems comparable based on results of existing clinical trials,[8–11] causing our difficulties for the treatment choices in real-world clinical practice. Until now, there has been no head-to-head study comparing the efficacy and safety of NAC, NICB, and NAC.NICB in the same real-world clinical setting. Moreover, the role of combination therapy in patients with unresectable or metastatic MIBC remains uncertain.[12,13] A multi-center randomized phase III trial (IMvigor130) demonstrated that addition of atezolizumab to platinum-based chemotherapy as first-line treatment significantly prolonged survival of patients when compared with chemotherapy alone.[13] In contrast, another randomized phase III trial (KEYNOTE-361) suggested that addition of pembrolizumab to first-line platinum-based chemotherapy did not significantly improve efficacy or survival, and it indicated that the combination therapy should not be widely adopted for advanced MIBC.[12] These ununified results further highlight the need for performing a real-world cohort study to explore the superiority of combination therapy compared with chemotherapy or immunotherapy alone. Second, robust biomarkers to predict treatment efficacy of neoadjuvant treatments are still lacking for MIBC. Third, the role of those emerging anti-PD-1/PD-L1 drugs, like tislelizumab, remains to be further investigated in the neoadjuvant settings, especially for the Chinese populations. Tislelizumab is a humanized monoclonal antibody with higher binding affinity to the PD-1 receptor than the common anti-PD-1 drugs, such as pembrolizumab and nivolumab.[14,15] The second advantage of tislelizumab is the ability to minimize its binding to the Fcγ receptor on macrophages and avoid antibody-dependent phagocytosis, which is a mechanism of T cell clearance and potential resistance to anti-PD-1 therapy.[15,16] Another significant advantage of tislelizumab was the lower price compared with other anti-PD-L1/PD-1 drugs.

Current clinical trials demonstrated that tislelizumab significantly improved the prognosis of several advanced malignancies, including MIBC.[16–18] Moreover, the combination of tislelizumab and chemotherapy resulted in superior survival benefits with similar side effects compared with chemotherapy alone.[19–21] Based on these promising results, tislelizumab has been approved in China.[18]

Here, we performed this real-world study in fifteen territory medicine centers to parallelly compare the efficacy and safety of NAC, NICB, and NAC.NICB in patients with MIBC, and we also explored the potential treatment efficacy predictors. This study assessed the efficacy and safety of tislelizumab in the neoadjuvant settings (NICB or NAC.NICB) for patients with MIBC.

RESULTS

Neoadjuvant treatment cohorts

As shown in Figure 1, we included patients from two stages, including discovery stage (n = 104; NAC.NICB: 30, NAC: 53, NICB: 21) and validation stage (n = 149; NAC.NICB: 68, NAC: 54, NICB: 27). Overall, 253 eligible patients with MIBC were included in our real-world cohorts, including NAC.NICB cohort (n = 98), NAC cohort (n = 107), and NICB cohort (n = 48). Overall, the baseline characteristics between these three cohorts were comparable, except for the age and Scr clearance rate (Table 1). Notably, the proportion of advanced clinical stage

Table 1. Patients baseline characteristics

	Overall (N = 253)	NAC.NICB (N = 98)	NAC (N = 107)	NICB (N = 48)	p value
Age (years)					0.001
Mean (SD)	62.5 (10.1)	60.5 (9.43)	62.4 (9.76)	67.0 (10.7)	
Scr clearance rate					0.019
Median (IQR)	68.3 (54.3, 83.9)	65.9 (56.1, 81.4)	74.9 (54.9, 89.5)	63.5 (45.4, 74.3)	
Sex					0.521
Female	43 (17.0%)	18 (18.4%)	15 (14.0%)	10 (20.8%)	
Male	210 (83.0%)	80 (81.6%)	92 (86.0%)	38 (79.2%)	
BMI					0.138
Mean (SD)	23.2 (3.13)	23.6 (3.33)	23.0 (3.05)	22.6 (2.81)	
Previous NMIBC					0.392
No	207 (81.8%)	84 (85.7%)	86 (80.4%)	37 (77.1%)	
Yes	46 (18.2%)	14 (14.3%)	21 (19.6%)	11 (22.9%)	
Previous BCG instillations					0.263
No	238 (94.1%)	95 (96.9%)	98 (91.6%)	45 (93.8%)	
Yes	15 (5.9%)	3 (3.1%)	9 (8.4%)	3 (6.3%)	
Smoking status					0.968
Nonsmoker	144 (56.9%)	55 (56.1%)	61 (57.0%)	28 (58.3%)	
Smoker	109 (43.1%)	43 (43.9%)	46 (43.0%)	20 (41.7%)	
Hydronephrosis					0.889
No	186 (73.5%)	73 (74.5%)	77 (72.0%)	36 (75.0%)	
Yes	67 (26.5%)	25 (25.5%)	30 (28.0%)	12 (25.0%)	
Grade					0.486
High grade	205 (81.0%)	82 (83.7%)	83 (77.6%)	40 (83.3%)	
Low grade	48 (19.0%)	16 (16.3%)	24 (22.4%)	8 (16.7%)	
Histology variants					0.387
UC	224 (88.5%)	85 (86.7%)	95 (88.8%)	44 (91.7%)	
SCC	19 (7.5%)	6 (6.1%)	10 (9.3%)	3 (6.3%)	
Sarcomatoid	4 (1.6%)	4 (4.1%)	0 (0%)	0 (0%)	
Neuroendocrine	6 (2.4%)	3 (3.1%)	2 (1.9%)	1 (2.1%)	
Clinical Stage					0.784
T2N0M0	141 (55.7%)	53 (54.1%)	61 (57.0%)	27 (56.3%)	
T3N0M0	61 (24.1%)	23 (23.5%)	24 (22.4%)	14 (29.2%)	
>T3N0M0	51 (20.2%)	22 (22.4%)	22 (20.6%)	7 (14.6%)	
Surgery					0.699
Partial cystectomy	2 (0.8%)	1 (1.0%)	1 (0.9%)	0 (0%)	
RC + ileal conduit	108 (42.7%)	43 (43.9%)	49 (45.8%)	16 (33.3%)	
RC + orthotopic neobladder	9 (3.6%)	4 (4.1%)	4 (3.7%)	1 (2.1%)	
RC + ureterocutaneostomy	101 (39.9%)	35 (35.7%)	43 (40.2%)	23 (47.9%)	
TURBT	33 (13.0%)	15 (15.3%)	10 (9.3%)	8 (16.7%)	

BMI: body mass index; TURBT: transurethral resection of the bladder tumor; NMIBC: non-muscle-invasive bladder cancer; BCG: Bacillus Calmette-Guerin; UC: urothelial carcinoma; SCC: squamous cell carcinoma; RC: radical cystectomy; SD: standard deviation; IQR: inter-quartile range; Scr: serum creatinine.

(>T3N0M0) in the whole real-world cohort (n = 253) reached 20.2%, which was significantly higher than that of previous clinical trials.[8,9,22,23] 33 patients refused RC and then received maximal TURBT because of strong personal preference for high quality of life, and two patients underwent partial cystectomy because of radiological progression and metastasis after two treatment cycles.

Efficacy and safety of three neoadjuvant treatments in our real-world settings

All 253 patients were evaluable for pathological staging, and the efficacy outcomes are summarized in Table 2. Among the overall cohort (n = 253), 50 patients (19.8%) achieved complete response (CR: pT0N0M0), and 72 (28.5%) patients achieved partial response (PR: pTis, Ta, T1, N0M0). The overall

Table 2. Pathologic response of three neoadjuvant schedules

	Overall (N = 253)	NAC.NICB (N = 98)	NAC (N = 107)	NICB (N = 48)	p value
Pathological response					0.002
CR	50 (19.8%)	31 (31.6%)	12 (11.2%)	7 (14.6%)	
PR	72 (28.5%)	28 (28.6%)	34 (31.8%)	10 (20.8%)	
SD	100 (39.5%)	31 (31.6%)	43 (40.2%)	26 (54.2%)	
PD	31 (12.3%)	8 (8.2%)	18 (16.8%)	5 (10.4%)	
CR response					0.001
CR	50 (19.8%)	31 (31.6%)	12 (11.2%)	7 (14.6%)	
Non-CR	203 (80.2%)	67 (68.4%)	95 (88.8%)	41 (85.4%)	
Binary response					0.007
Responder (CR + PR)	122 (48.2%)	59 (60.2%)	46 (43.0%)	17 (35.4%)	
Nonresponder (SD + PD)	131 (51.8%)	39 (39.8%)	61 (57.0%)	31 (64.6%)	
DCR response					0.153
DCR	222 (87.7%)	90 (91.8%)	89 (83.2%)	43 (89.6%)	
Non-DCR	31 (12.3%)	8 (8.2%)	18 (16.8%)	5 (10.4%)	

NAC.NICB: combination of neoadjuvant chemotherapy and immunotherapy; NAC: neoadjuvant chemotherapy; NICB: neoadjuvant immunotherapy; CR: complete response; PR: partial response; SD: stable disease; PD: progression disease. DCR: disease control rate.

pathologic downstaging rate (<pT2N0M0: responder) and disease control rate (DCR) were 48.2% and 87.7%, respectively. 31 patients (12.3%) presented with progression diseases (PD).

Three different neoadjuvant treatments were carried out at the same real-world setting and had comparable baseline characteristics, which allowed us to head-to-head compare their efficacy and safety. Obviously, patients in NAC.NICB cohort achieved significantly higher CR rate than another two cohorts (31.6% vs. 11.2% and 14.6% respectively, p = 0.001). Similarly, the pathological downstaging rate of NAC.NICB (60.2%) was significantly higher than that of NAC cohort (43.0%) and NICB cohort (35.4%) (p = 0.007). As for the DCR, there was no difference between these three neoadjuvant schedules (p = 0.153).

During the discovery stage, a total of 84 patients could be followed up with well. Overall, patients achieving pathological downstaging (responders) had significantly higher overall survival (OS) rates compared with non-responders (Figure S1A). A similar result was observed in the NAC subgroup (Figure S1B). It is worth noting that the median OS had not been reached in the NAC.NICB cohort and the NICB cohort. Although the death events of non-responders were more than that of responders, the difference was not statistically significant (Figures S1C and S1D). Overall, we demonstrated that the pathological response might be a surrogate marker for OS. The treatment-related adverse events (TRAEs) were able to be analyzed in 21 patients from NAC.NICB and nine patients from NICB cohorts (Table S1). Obviously, the frequencies of TRAEs were higher in NAC.NICB cohort compared with NICB cohort. In NAC.NICB cohort, the most common TRAEs were nausea (47.6%) and pruritus (42.9%). Grade 3 TRAEs included anemia, decreased neutrophil count, decreased platelet count, nausea, and hypothyroidism. In NICB cohort, the TRAE frequencies were low. But a grade 4 TRAE (hypothyroidism) occurred in one patient.

Associations between clinicopathological characteristics and pathological response

We focused on NAC.NICB cohort to screen biomarkers for predicting treatment response because of the highest CR and pathological response rates in this cohort. A total of 28 patients had enough pretreatment clinicopathological features to be analyzed during the discovery stage. Univariable analyses of all available clinicopathological variables between responders and non-responders are presented in Table S2 (variables with $p > 0.1$) and Table 3 (variables with $p < 0.1$). 9 of 11 patients (81.81%) achieved pathologic response in T2N0M0 subgroup, while this rate was only 29.41% (5 of 17 patients) in >T2N0M0 subgroup (p = 0.018). Patients with pure urothelial carcinoma (UC) possessed significantly higher pathological response rates than patients with histology variants (63.64% vs. zero). In addition, patients in the pathological response group had higher levels of hemoglobin but lower levels of platelet, globulin, and platelet-to-lymphocyte ratio (PLR). However, the neoadjuvant treatment sequence (p = 0.077) was not related to pathological response. In summary, lower clinical stage (p = 0.018), pure UC histology (p = 0.016), higher hemoglobin (p = 0.019), lower platelet (p = 0.044), lower globulin (p = 0.034), and lower PLR (p = 0.016) were significantly associated with higher pathological response rates.

Development and validation of a pathological response prediction model based on pure pretreatment clinical characteristics in the NAC.NICB cohort

Five pure pretreatment clinical characteristics, including clinical stage and four hematologic characteristics, were significantly associated with pathological response. However, because of the small sample size during the discovery stage, we had to reduce the number of variables to avoid model overfitting. Interestingly, there were obvious linear relationships between four hematologic characteristics (Figure 2A). Based on the relationships between these four indicators and pathological response,

Table 3. Univariate analysis of pathological response-related factors of NAC.NICB cohort during the discovery stage

	Overall (N = 28)	Nonresponder (N = 14)	Responder (N = 14)	p value
Clinical stage				0.018
T2N0M0	11 (39.3%)	2 (14.3%)	9 (64.3%)	
>T2N0M0	17 (60.7%)	12 (85.7%)	5 (35.7%)	
Histology variants				0.016
Pure UC	22 (78.6%)	8 (57.1%)	14 (100%)	
UC with SCC (>10%)	5 (17.9%)	5 (35.7%)	0 (0%)	
Sarcomatoid	1 (3.6%)	1 (7.1%)	0 (0%)	
Neoadjuvant treatment sequence				0.077
NAC-before-NICB	4 (14.3%)	4 (28.6%)	0 (0%)	
NICB-before-NAC	7 (25.0%)	2 (14.3%)	5 (35.7%)	
NICB-concur-NAC	17 (60.7%)	8 (57.1%)	9 (64.3%)	
Erythrocyte				0.081
Median [IQR]	4.12 [3.79, 4.54]	3.91 [3.78, 4.28]	4.36 [4.03, 4.80]	
Hemoglobin				0.019
Mean (SD)	128 (19.2)	120 (19.1)	137 (15.6)	
Platelet				0.044
Median [IQR]	210.00 [179.00, 265.00]	212.50 [195.50, 334.00]	185.00 [160.00, 232.00]	
Globulin				0.034
Mean (SD)	28.1 (4.70)	29.9 (5.02)	26.1 (3.55)	
NSE				0.054
Mean (SD)	5.03 (3.79)	6.62 (4.48)	2.99 (0.742)	
PLR				0.016
Mean (SD)	146 (62.1)	173 (69.3)	117 (37.4)	
ALG				0.057
Mean (SD)	1.40 (0.263)	1.31 (0.267)	1.50 (0.228)	

UC: urothelial carcinoma; SCC: squamous cell carcinoma; PLR: platelet-to-lymphocyte ratio; ALG: albumin-to-globulin ratio: NAC.NICB: combination of neoadjuvant chemotherapy and immunotherapy; NAC: neoadjuvant chemotherapy; NICB: neoadjuvant immunotherapy.

we integrated them into a new indicator, named PLR.GHR (PLR*Globulin/Hemoglobin). As expected, the PLR.GHR was significantly higher in non-responders than responders (Figure 2B). Moreover, PLR.GHR possessed the highest predictive accuracy for pathological response (AUC = 0.80) compared with four indicators alone (Figure 2C). These results were successfully tested during the validation stage (Figures S2A–S2C). We then incorporated the clinical stage and PLR.GHR into a multivariate logistic regression model and developed a nomogram (Figure 2D). The response scores of all patients calculated by the nomogram are listed in Figures 2E and S2D. The bootstrapped AUC of the nomogram was 0.95, which was higher than those of the clinical stage (AUC = 0.77) and PLR.GHR (AUC = 0.80) (Figure 2F). The calibration curve analysis showed that the predicted response sensitivity was consistent with the actual response sensitivity (Figure 2G). Finally, decision curve analysis demonstrated that the net benefit of the nomogram was obviously higher than those of the "treat-all" scheme, "treat-none" scheme, PLR.GHR, and clinical stage (Figure 2H).

Then, we tested the statistical performance of the nomogram during the validation stage. As expected, the predictive accuracy of the nomogram reached 0.83, which was acceptable and was higher than those of the clinical stage (AUC = 0.65) and PLR.GHR (AUC = 0.80) (Figure 2I). In addition, the calibration curve analysis and decision curve analysis were well validated (Figures 2J and 2K).

Pathological response prediction with routine contrast-enhanced computed tomography after two neoadjuvant treatment cycles

In the NICB and NAC.NICB cohorts during the discovery stage, 28 patients had baseline computed tomography (CT) before neoadjuvant treatment and comparable CT with the same parameters after two neoadjuvant treatment cycles. We evaluated the radiographic response after two treatment cycles according to the RECIST-criteria (response evaluation criteria in solid tumors). Meanwhile, we evaluated the pathologic-clinic response and divided patients into CR (pT0N0M0), PR (patients with lower pathological stage than clinical stage), stable disease (SD; patients with equal pathological stage and clinical stage), and PD (patients with higher pathological stage than clinical stage) groups.[24]

Figures S3A–S3F show the one-to-one correspondence of radiographic response, pathological response, and pathologic-clinic response. Obviously, a considerable part of patients with radiographic PR were confirmed as pathological SD or PD, especially in the NAC.NICB cohort. Overall, the radiographic response and pathologic-clinic response were notably

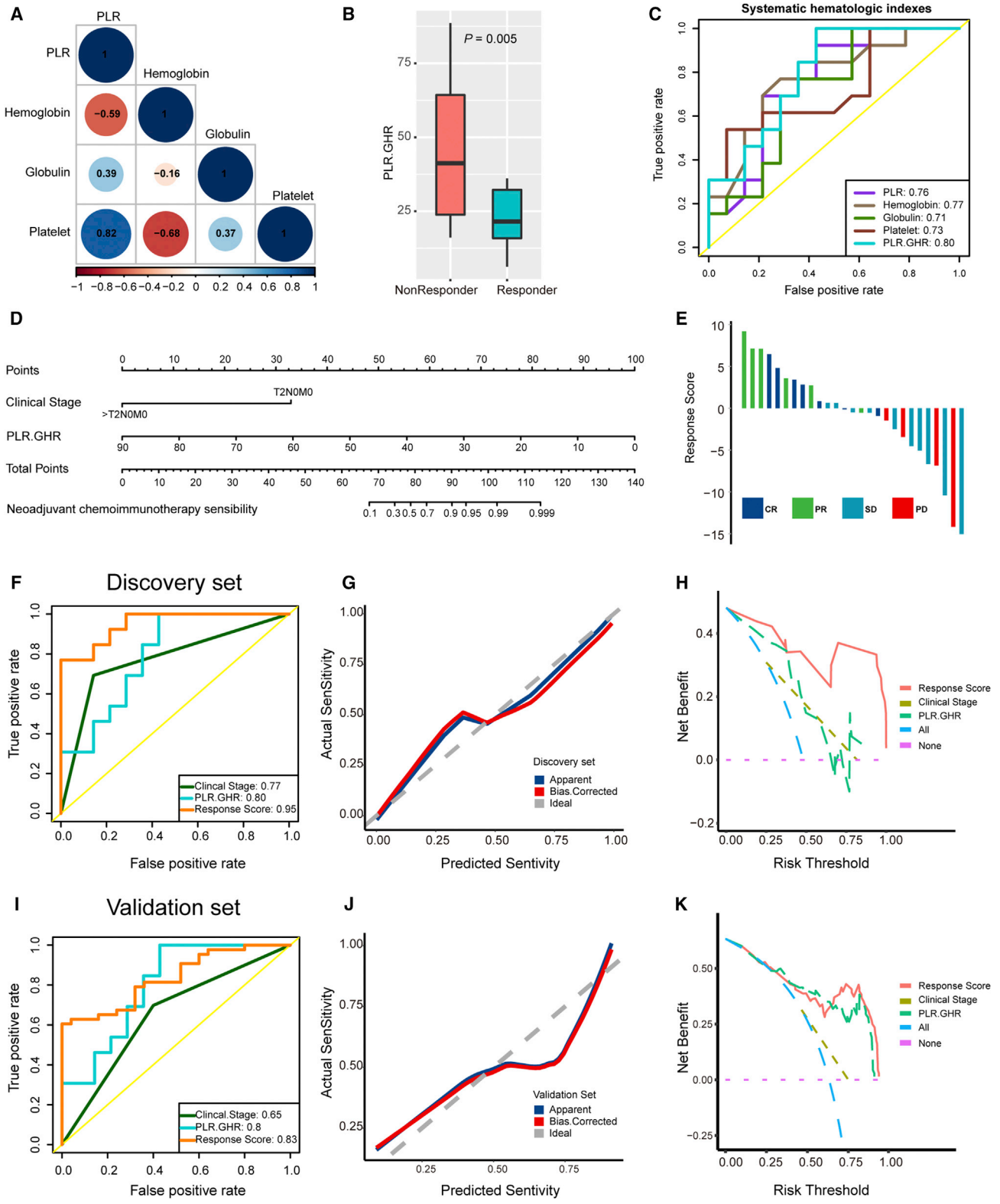

Figure 2. Developing and validating the pathological response prediction nomogram in the NAC.NICB cohort

(A) The spearman correlations between four hematological indicators during the discovery stage. Brown color represents negative correlation, while blue color represents positive correlation. PLR: platelet-to-lymphocyte ratio.

(legend continued on next page)

overestimated compared with the pathological response. As shown in Figure S3G, a considerable part of patients with pathological SD or PD had a decrease in the longest diameters. Overall, radiographic response after two treatment cycles could not accurately predict the pathological response in the NICB cohort (AUC = 0.75) or NAC.NICB cohort (AUC = 0.67) (Figure S3H).

Bladder preservation therapy in our real-world cohorts

Overall, 33 patients received bladder preservation therapy (maximal TURBT). All patients were followed up with well. The baseline characteristics of these 33 patients receiving bladder preservation therapy are listed in Table S3. Among them, 10 patients (30.3%) received NAC.NICB, 15 patients (45.5%) received NAC, and 8 patients (24.2%) received NICB. After a median follow-up of 13 months, 93.94% of patients (31 of 33) achieved disease-free survival. These patients benefited from a significantly improved quality of life after bladder preservation therapy without any recurrence or metastasis. The remaining two patients underwent intravesical recurrence: one of them (pT2N0M0) underwent recurrence at 11 months after NAC.NICB plus maximal TURBT and ICB maintenance treatment, and the other patient (pT1N0M0) had a recurrence at 12 months and died at 19 months after receiving NAC plus maximal TURBT and chemoradiotherapy maintenance treatment. We did not identify any risk factors for intravesical recurrence after bladder preservation therapy (Table S3). However, it was worth noting that both patients with recurrence were non-CR ($p = 0.055$).

Biomarker analysis for the efficacy of neoadjuvant treatments based on tislelizumab in BLCA

In NAC.NICB cohort, we filtered out 308 differentially expressed genes (DEGs) between response and resistance samples (Table S4), and these DEGs were mainly enriched in extracellular matrix in gene ontology (GO) analysis (Figure 3A and Table S5). Several KEGG pathways, including MAPK signaling, TNF signaling, and IL-17 signaling pathway were enriched based on these DEGs (Figure 3B and Table S5). As shown in Figure 3C, the cytokine-cytokine receptor interaction pathway (a signature associated with ICB resistance) was obviously enriched in the resistance samples.[25] Consistently, another 17 signatures associated with ICB response were obviously enriched in the response samples. However, there was no significant difference between response and resistance samples regarding the infiltration level of tumor-associated immune cells and the expression of PD-L1 and PD-1 (Figure S4). The enrichment scores of four stromal signatures were higher in resistance samples, though the differences did not reach statistical significance (Figure 3D). Interestingly, the enrichment score of the NAC response signature was significantly higher in response group than that in resistance group (Figure 3E).

In NICB cohort, we further explored the potential efficacy biomarkers from the single-cell RNA-seq level. As shown in Figure S5A, a total of 16,298 qualified single cells were classified into 17 clusters. These clusters were further defined into seven cell types, including bladder cancer epithelial cell, endothelial cell, T/NK cell, myeloid cell, B cell, fibroblast cell, and others (Figures S5B–S5I). Obviously, there was high heterogeneity between NICB response and resistance samples (Figures S5J–S5K). We compared the differences on the counts and proportions of all cell types between NICB response and resistance samples (Figures S5L–S5M). The results indicated that cancer cells and T/NK cells may be determinants for NICB response in BLCA. Therefore, we further classified the T/NK cells into three subgroups, including CD8 T cells, CD4 T cells, and NK cells (Figures S6A–S6J). As expected, the number of T/NK cells of NICB resistance group was smaller than that of NICB response group (Figure S6K). Especially, the proportions of CD8 T cells and NK cells were lower in NICB resistance group (Figure S6L), which highlighted the critical role of CD8 T cells and NK cells for NICB response.

As for the bladder cancer cells, we further classified them into five clusters (Figure 4A). Then, we explored the functions of these clusters based on their over-expressed genes. As shown in Figure 4B, the functions of Cluster 0 mainly enriched in neutrophil-related pathways. The functions of Cluster 1 enriched in RNA catabolic-related pathways (Figure 4C). The functions of Cluster 2 and Cluster 3 enriched in RNA splicing-related pathways (Figures 4D and 4E). The functions of Cluster 4 enriched in cell cycle-related pathways (Figure 4F). Therefore, these five clusters were annotated into four subtypes, including neutrophil subtype (Cluster 0), RNA catabolic subtype (Cluster 1), RNA splicing subtype (Cluster 2 and Cluster 3), and cell cycle subtype (Cluster 4) (Figure 4G). Obviously, the cell cycle subtype is a unique cell subtype in the NICB response group (Figure 4H). There was no difference in the other three subtypes between NICB resistance and response groups. Meanwhile, the results of gene set enrichment analysis (GSEA) analysis further validated the robustness of this cell cycle subtype (Figure S7A). Furthermore, we demonstrated that several critical immune-related pathways, such as antigen processing and presentation, chemokine-related pathway, and T cell-related pathway, were significantly enriched in cell cycle subtypes (Figure S7B). More importantly, 18 signatures associated with ICB response were obviously enriched in the cell cycle subtypes, while the pathway associated with ICB resistance (cytokine-cytokine receptor interaction pathway)

(B) The PLR.GHR level in responders and non-responders during the discovery stage.
(C) Receiver operating characteristic (ROC) curves of five hematological indicators for predicting pathological response during the discovery stage.
(D) The pathological response prediction nomogram during the discovery stage.
(E) Bar plots show the distribution of response scores calculated by the nomogram in different response groups during the discovery stage.
(F) ROC curves of clinical stage, PLR.GHR, and response scores for predicting pathological response during the discovery stage.
(G) The calibration curves show that the predicted response sensitivity was consistent with the actual sensitivity during the discovery stage.
(H) The decision curves highlight the highest net benefit of response score compared with clinical stage and PLR.GHR during the discovery stage.
(I) ROC curves of clinical stage, PLR.GHR, and response score for predicting pathological response during the validation stage.
(J) The calibration curves show that the predicted response sensitivity was consistent with the actual sensitivity during the validation stage.
(K) The decision curves highlight the highest net benefit of response score compared with clinical stage and PLR.GHR during the validation stage.

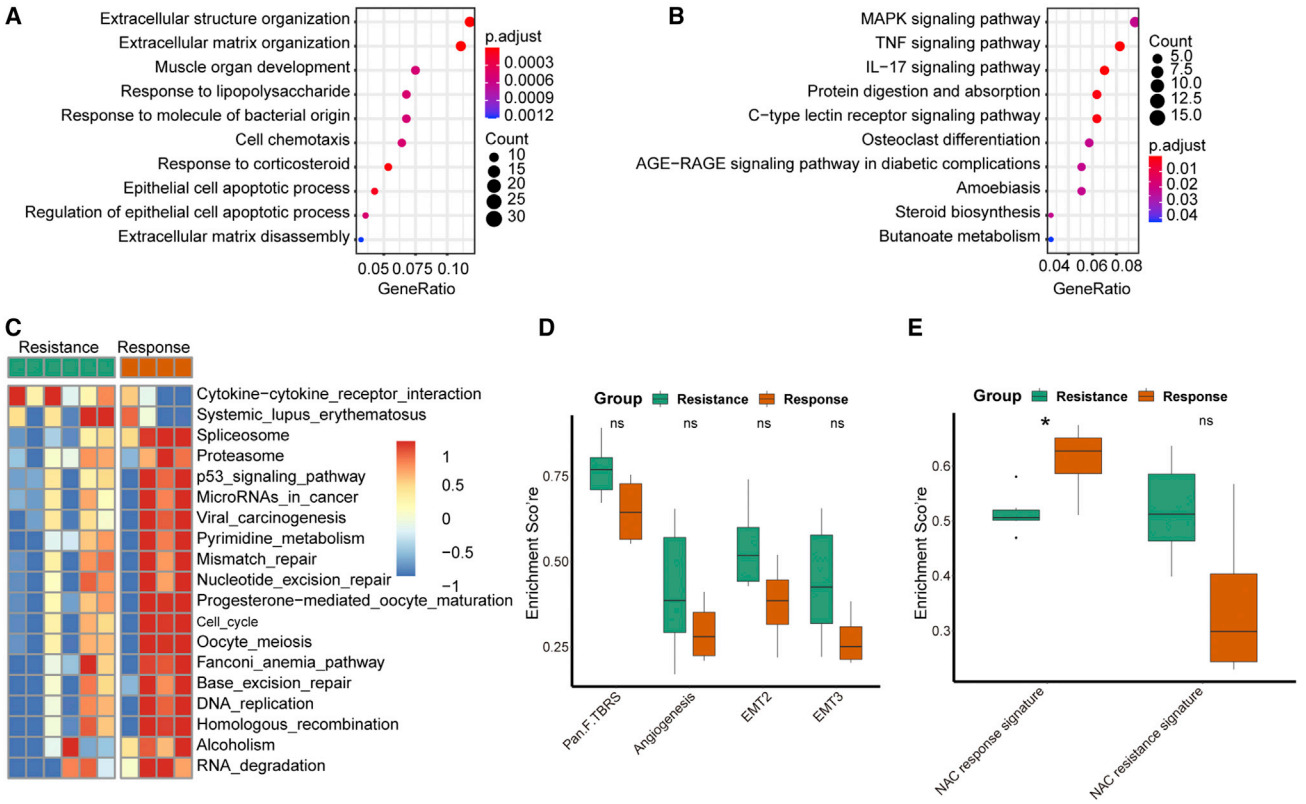

Figure 3. Biomarker analysis of pathological response in the NAC.NICB cohort

(A) GO and (B) KEGG analysis of differentially expressed genes between response and resistance samples. The enrichment score distribution patterns of (C) 19 immunotherapy efficacy associated signatures, (D) four stromal signatures, and (E) two NAC efficacy associated signatures between response and resistance samples.

was significantly enriched in other cancer cells (Figure S7C). Consistently, previous studies have shown that abnormal changes in cell cycle-related pathways may increase the level of tumor mutation burden (TMB) and neoantigen in the tumor microenvironment, thereby increasing tumor immunogenicity and sensitivity to immunotherapy.[25–28] In summary, we identified a cluster of special cancer cells, called cell cycle subtype, that were critical for the NICB response in BLCA.

DISCUSSION

Although the efficacy of neoadjuvant chemotherapy has been well confirmed, only a few prospective clinical trials have demonstrated the efficacy and safety of neoadjuvant immunotherapy or neoadjuvant immunochemotherapy.[8–11] More importantly, the generalizability of findings derived from these well-selected clinical trials to real-world settings remains unclear.[29,30] The current study compared the efficacy of three neoadjuvant treatments head to head in the same real-world clinical practice setting. Meanwhile, we assessed the role of tislelizumab in the neoadjuvant settings (NICB or NAC.NICB) for patients with MIBC. The overall pathological downstaging rate (48.2%) in our real-world cohort was comparable to that of previous clinical trials.[11,31] The overall CR rate (19.8%) was lower than previous trials (28%–42%).[10,11,23,31] This lower CR rate was attributed to the higher proportion of patients with advanced stage (>T3N0M0) (20.2%), which has been proved to be a negative factor for pathological response.[8,10,32] The proportion of patients with advanced stage ranged from 1.8% to 5% in previous prospective clinical trials, including PRE-01, BLASST-1, and ABACUS studies.[8–11,22,33]

The comparable baseline characteristics between three neoadjuvant treatments allowed us to head-to-head compare their efficacy and safety. The CR rate (31.6%) and pathological downstaging rate (60.2%) in our real-world NAC.NICB cohort were comparable to that of prior prospective clinical trials of NAC.NICB (30%–36% for CR; 50%–66% for pathological downstaging rate) in patients with MIBC,[10,22,23] despite a significantly higher proportion of patients with advanced stage in our cohort (>T3N0M0). However, the CR rate (14.6%) and pathological downstaging rate (35.4%) were lower in our real-world NICB cohort when compared with prior NICB clinical trials (31%–37.5% for CR; 58% for pathological downstaging rate).[8,9,32,33] Similarly, the CR rate of our real-world NAC cohort (11.2%) was lower than CR (30%–36%) of previous trials, despite that the pathological downstaging rates were comparable (40%–49%).[11,31] Although the TRAEs frequencies were higher in the NAC.NICB cohort compared with the NICB cohort, there

CellPress
OPEN ACCESS

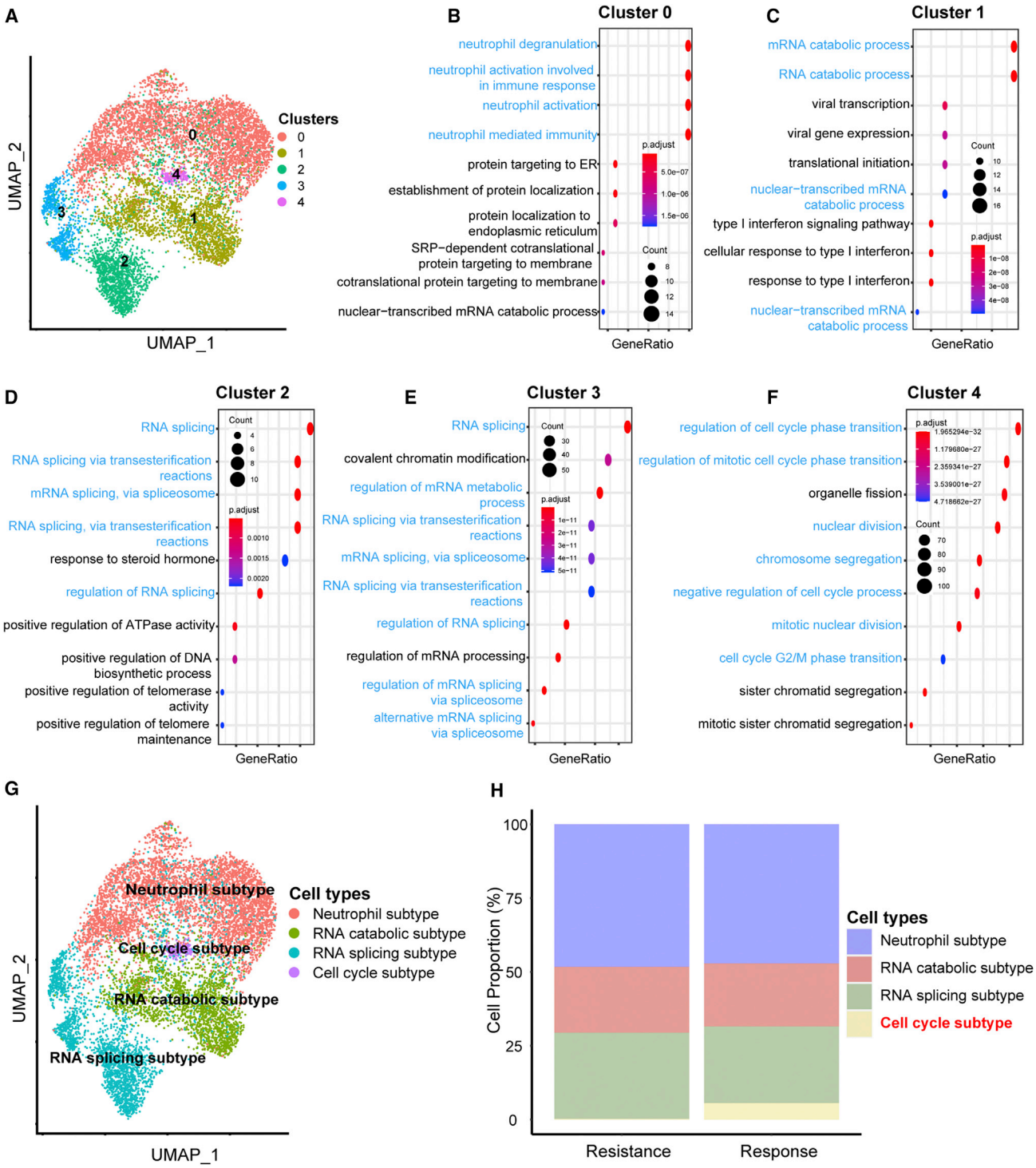

Figure 4. Reclustering of bladder cancer cells in the NICB cohort

(A) UMAP plot of subgroups of bladder cancer cells.

(B–F) The most enriched functions of clusters 0–5.

(G) UMAP plot of four bladder cancer subtypes.

(H) Histogram indicating the proportions of four bladder cancer subtypes of NICB resistance and response groups.

was no grade 4 TRAE in the NAC.NICB cohort. In summary, NAC.NICB, composed of GC and tislelizumab, achieved the highest CR rate and pathological downstaging rate, compared with NICB and NAC alone in the same real-world clinical practice setting. However, the advantages of combination therapy over chemotherapy alone for metastatic MIBC have not been recognized. Two phase III trials, including IMvigor130 and KEYNOTE-361, revealed contrasting conclusions despite a similarity in hazard ratios.[12,13] IMvigor130 study demonstrated that combination therapy significantly improved the progression-free survival of patients with metastatic MIBC, while KEYNOTE-361 trial did not meet the primary endpoints of superior progression-free survival or overall survival with combination therapy versus chemotherapy alone. The differences between these studies and our real-world cohort study may be attributed to several reasons, such as the type of study design, different statistical assumptions, and different immunotherapy drugs.

So far, there was no robust biomarker to predict the treatment efficacy of NAC.NICB. Our study explored the potential predictors for the efficacy of NAC.NICB in a real-world setting. Consistent with previous trials, the clinical stage was an efficacy predictor in our real-world NAC.NICB cohort.[8,10,32] In addition, several hematological indicators reflecting the systematic inflammation, including hemoglobin, platelet, globulin, and PLR, were associated with NAC.NICB efficacy.[34,35] These pretreatment hematological indicators were more accessible, economical, and repeatable than biomarkers derived from cancer tissues. In order to develop an efficacy prediction model without overfitting, we defined a new comprehensive indicator, named PLR.GHR, based on four hematological indicators. The PLR.GHR had the highest accuracy to predict NAC.NICB efficacy compared with four baseline hematological indicators. Finally, we developed and validated a nomogram with superior statistical performances by incorporating two pure clinical variables: clinical stage and PLR.GHR. More importantly, the clinical value and statistical performance of this nomogram were well validated.

The administration of antibiotics during NICB compromised therapeutic efficacy in the PURE-01 study.[36] But in our NAC.NICB and NICB cohorts, we did not find any relationship between the usage of concomitant antibiotics and efficacy. Chemotherapy could increase the immunogenicity of tumor microenvironment (TME) by inducing more immunogenic cell death and releasing more cytokines.[37] Consistently, Xing et al. demonstrated that the application of anti-PD-1 antibody 2 days after chemotherapy (NAC-before-NICB) achieved a higher CR rate than that on the same day (NAC-concur-NICB).[38] The current NAC.NICB clinical trials for MIBC, including BLASST-1 and SAKK 06/17 studies, applied the NAC-before-NICB mode.[22,23,33] However, we found that the neoadjuvant treatment sequence was not related to the response rate. Therefore, the optimal sequence of immunotherapy and chemotherapy in the neoadjuvant setting remains to be further explored in future clinical trials. Recently, Patel et al. reported that three cycles (short course) of neoadjuvant treatment achieved similar pathologic response rates and comparable short-term survival compared with four cycles (long course).[2] In contrast, D'Andrea et al. demonstrated that a long course achieved better pathological response rate and prolonged survival compared with a short course. In our real-world cohorts, there was no association between the treatment cycles and outcomes regardless of treatment regimens (Table S6). It is worth noting that a long course will delay RC; whether this will impair the long-term survival needs further evaluation. PD-L1 was proven to be an efficacy predictor for adjuvant immunotherapy or NICB in patients with MIBC.[9,25] However, the previous NAC.NICB trials suggested that baseline PD-L1 was not related to the pathological response,[10,22] which was confirmed in our NAC.NICB cohort. As for the NICB, we identified a cluster of "cell cycle subtype" bladder cancer cells, which were positive determinants for NICB efficacy, from the single-cell RNA-seq level.

The addition of NAC to conventional trimodality therapy extended the clinical application of bladder preservation therapy for selected patients with MIBC.[39–41] Compared with NAC, NICB and NAC.NICB might significantly reactivate and increase the anti-cancer immunity of peripheral blood and tumor microenvironment, thereby eliminating the micro-metastatic tumor and circulating tumor cells that could result in postoperative recurrence.[42,43] Theoretically, NICB and NAC.NICB may be more suitable for bladder preservation therapy than NAC. In our real-world cohorts, 33 patients received bladder preservation therapy due to strong personal preference for high quality of life and were followed up with well. Overall, 93.94% of patients (31 of 33) achieved disease-free survival during a median follow-up of 13 months. Especially for 18 patients receiving NAC.NICB or NICB followed by bladder preservation therapy, the rate of intact bladder preservation without recurrence reached 94.44%, which was superior to other trials.[39,41,44,45] Two points are worth highlighting concerning the high rate of intact bladder preservation in our real-world cohorts. First, the follow-up period was short. Second, all patients received maximal TURBT after completing neoadjuvant treatments, regardless of the radiographic response. The maximal TURBT could resect the micro-residual cancer tissues in patients misdiagnosed as clinical CR.

We found that pathological non-CR seems to be correlated with intravesical recurrence ($p = 0.055$). Patients who achieved CR had more favorable survival outcomes after bladder preservation therapy.[39] Therefore, it was critical to predict CR before receiving bladder preservation therapy. In our real-world clinical practice setting, contrast-enhanced CT was the most commonly used method for predicting pathological response. Unfortunately, we found that CT could not accurately predict the pathological response. Many patients with pathological SD or PD were defined as radiographic PR. A similar phenomenon was reported in several previous studies.[46,47] Therefore, routine control CT could not be used to select patients to receive bladder preservation therapy; instead, multiparametric magnetic resonance imaging may be an alternative method.[48] Compared with these subjective radiographic methods, more objective biomarkers are needed to pinpoint the candidates who can safely receive bladder preservation therapy; several biomarkers-guided trials selecting patients with DNA repair genes defection to receive bladder preservation therapy, including the RETAIN and the HCRN GU 16–257 studies, are ongoing.[40,41]

In conclusion, neoadjuvant chemoimmunotherapy, composed of GC and tislelizumab, achieved the highest CR rate and pathological downstaging rate, compared with neoadjuvant

chemotherapy and neoadjuvant immunotherapy alone in the same real-world clinical practice setting; Neoadjuvant chemoimmunotherapy could be safely administered in patients with MIBC. An efficacy prediction model was developed and validated to aid in pinpointing candidates to receive neoadjuvant chemoimmunotherapy. During a short-term follow-up period, patients who achieved pathological CR after neoadjuvant treatments plus maximal TURBT may be safe to receive bladder preservation therapy.

Limitations of the study

Several limitations existed in our real-world study. First, this is a real-world retrospective cohort study with some inevitable bias. Fortunately, the baseline characteristics between three cohorts were comparable, which indicated the patient selection bias was acceptable. Second, the follow-up periods of the NAC.NICB and NICB cohorts were short. Third, the sample size of the discovery stage was small. Fourth, the sample size of biomarker analysis should be further expanded.

STAR★METHODS

Detailed methods are provided in the online version of this paper and include the following:

- KEY RESOURCES TABLE
- RESOURCE AVAILABILITY
  - Lead contact
  - Materials availability
  - Data and code availability
- EXPERIMENTAL MODEL AND SUBJECT DETAILS
  - Ethics statement
  - Human subjects
- METHOD DETAILS
  - Study design, outcomes and patient selection
  - Neoadjuvant treatment schedules
  - Clinicopathological characteristics collection and definition
  - Biomarker analysis
- QUANTIFICATION AND STATISTICAL ANALYSIS

SUPPLEMENTAL INFORMATION

Supplemental information can be found online at https://doi.org/10.1016/j.xcrm.2022.100785.

ACKNOWLEDGMENTS

We sincerely thank all participants in the study. We sincerely thank Jianhao Wu for helping us collect data. We thank OE Biotech Co., Ltd., (Shanghai, China) for providing single-cell RNA-seq and Dr. Yongbing Ba, Yao Lu, and Hengyun Wang for assistance with bioinformatics analysis. This work was supported by the National Natural Science Foundation of China (81873626, 81902592, 82070785), Hunan Natural Science Foundation (2020JJ5884, 2020JJ5916), and Hunan Province Young Talents Program (2021RC3027).

AUTHOR CONTRIBUTIONS

H.J., L.H.H., L.J.H., C.J.B., O.B., and C.C.L. performed analyses and drafted the manuscript. H.J., C.J.B., O.Z.Y., C.H.G., L.Z., C.M.F., Z.R.B., Y.A.Z., C.R., Z.E.C., G.X., P.B., L.H.H., L.J.H., C.M.F., C.C.L., Z.C.Y., C.Z.Y., L.Z., D.R.P., Q.G., L.W.Z., W.L., C.T., P.X.M., and T.J.S. contributed to data collecting and statistical analyses. H.J., L.H.H., C.C.L., O.Z.Y., and D.D.S. edited the pictures. Z.X.B. and C.J.B. conceived and supervised the study. All authors contributed to writing the manuscript. All authors reviewed and approved the final manuscript.

DECLARATION OF INTERESTS

The authors declare that they have no competing interests.

Received: February 28, 2022
Revised: June 29, 2022
Accepted: September 24, 2022
Published: October 19, 2022

REFERENCES

1. Griffiths, G., Hall, R., Sylvester, R., Raghavan, D., and Parmar, M.K. (2011). International phase III trial assessing neoadjuvant cisplatin, methotrexate, and vinblastine chemotherapy for muscle-invasive bladder cancer: long-term results of the BA06 30894 trial. J. Clin. Oncol. *29*, 2171–2177. https://doi.org/10.1200/jco.2010.32.3139.
2. Patel, H.D., Patel, S.H., Blanco-Martinez, E., Kuzbel, J., Chen, V.S., Druck, A., Koehne, E.L., Patel, P.M., Doshi, C.P., Hahn, N.M., et al. (2022). Four versus 3 cycles of neoadjuvant chemotherapy for muscle-invasive bladder cancer: implications for pathological response and survival. J. Urol. *207*, 77–85. https://doi.org/10.1097/ju.0000000000002189.
3. D'Andrea, D., Black, P.C., Zargar, H., Dinney, C.P., Soria, F., Cookson, M.S., Montgomery, J.S., Kassouf, W., Dall'Era, M.A., Sridhar, S.S., et al. (2022). Identifying the optimal number of neoadjuvant chemotherapy cycles in patients with muscle invasive bladder cancer. J. Urol. *207*, 70–76. https://doi.org/10.1097/ju.0000000000002190.
4. Burger, M., Mulders, P., and Witjes, W. (2012). Use of neoadjuvant chemotherapy for muscle-invasive bladder cancer is low among major European centres: results of a feasibility questionnaire. Eur. Urol. *61*, 1070–1071. https://doi.org/10.1016/j.eururo.2012.01.039.
5. Raj, G.V., Karavadia, S., Schlomer, B., Arriaga, Y., Lotan, Y., Sagalowsky, A., and Frenkel, E. (2011). Contemporary use of perioperative cisplatin-based chemotherapy in patients with muscle-invasive bladder cancer. Cancer *117*, 276–282. https://doi.org/10.1002/cncr.25429.
6. Necchi, A., Joseph, R.W., Loriot, Y., Hoffman-Censits, J., Perez-Gracia, J.L., Petrylak, D.P., Derleth, C.L., Tayama, D., Zhu, Q., Ding, B., et al. (2017). Atezolizumab in platinum-treated locally advanced or metastatic urothelial carcinoma: post-progression outcomes from the phase II IMvigor210 study. Ann. Oncol. *28*, 3044–3050. https://doi.org/10.1093/annonc/mdx518.
7. Powles, T., Durán, I., van der Heijden, M.S., Loriot, Y., Vogelzang, N.J., De Giorgi, U., Oudard, S., Retz, M.M., Castellano, D., Bamias, A., et al. (2018). Atezolizumab versus chemotherapy in patients with platinum-treated locally advanced or metastatic urothelial carcinoma (IMvigor211): a multicentre, open-label, phase 3 randomised controlled trial. Lancet (London, England) *391*, 748–757. https://doi.org/10.1016/s0140-6736(17)33297-x.
8. Powles, T., Kockx, M., Rodriguez-Vida, A., Duran, I., Crabb, S.J., Van Der Heijden, M.S., Szabados, B., Pous, A.F., Gravis, G., Herranz, U.A., et al. (2019). Clinical efficacy and biomarker analysis of neoadjuvant atezolizumab in operable urothelial carcinoma in the ABACUS trial. Nat. Med. *25*, 1706–1714. https://doi.org/10.1038/s41591-019-0628-7.
9. Necchi, A., Anichini, A., Raggi, D., Briganti, A., Massa, S., Lucianò, R., Colecchia, M., Giannatempo, P., Mortarini, R., Bianchi, M., et al. (2018). Pembrolizumab as neoadjuvant therapy before radical cystectomy in patients with muscle-invasive urothelial bladder carcinoma (PURE-01): an open-label, single-arm, phase II study. J. Clin. Oncol. *36*, 3353–3360. https://doi.org/10.1200/jco.18.01148.
10. Rose, T.L., Harrison, M.R., Deal, A.M., Ramalingam, S., Whang, Y.E., Brower, B., Dunn, M., Osterman, C.K., Heiling, H.M., Bjurlin, M.A., et al.

(2021). Phase II study of gemcitabine and split-dose cisplatin plus pembrolizumab as neoadjuvant therapy before radical cystectomy in patients with muscle-invasive bladder cancer. J. Clin. Oncol. *39*, 3140–3148. https://doi.org/10.1200/jco.21.01003.

11. Pfister, C., Gravis, G., Fléchon, A., Soulié, M., Guy, L., Laguerre, B., Mottet, N., Joly, F., Allory, Y., Harter, V., and Culine, S.; VESPER Trial Investigators (2021). Randomized phase III trial of dose-dense methotrexate, vinblastine, doxorubicin, and cisplatin, or gemcitabine and cisplatin as perioperative chemotherapy for patients with muscle-invasive bladder cancer. Analysis of the GETUG/AFU V05 VESPER trial secondary endpoints: chemotherapy toxicity and pathological responses. Eur. Urol. *79*, 214–221. https://doi.org/10.1016/j.eururo.2020.08.024.

12. Powles, T., Csőszi, T., Özgüroğlu, M., Matsubara, N., Géczi, L., Cheng, S.Y.S., Fradet, Y., Oudard, S., Vulsteke, C., Morales Barrera, R., et al. (2021). Pembrolizumab alone or combined with chemotherapy versus chemotherapy as first-line therapy for advanced urothelial carcinoma (KEYNOTE-361): a randomised, open-label, phase 3 trial. Lancet Oncol. *22*, 931–945. https://doi.org/10.1016/s1470-2045(21)00152-2.

13. Galsky, M.D., Arija, J.Á.A., Bamias, A., Davis, I.D., De Santis, M., Kikuchi, E., Garcia-Del-Muro, X., De Giorgi, U., Mencinger, M., Izumi, K., et al. (2020). Atezolizumab with or without chemotherapy in metastatic urothelial cancer (IMvigor130): a multicentre, randomised, placebo-controlled phase 3 trial. Lancet (London, England) *395*, 1547–1557. https://doi.org/10.1016/s0140-6736(20)30230-0.

14. Feng, Y., Hong, Y., Sun, H., Zhang, B., Wu, H., Li, K., Liu, X., and Liu, Y. (2019). The Molecular Binding Mechanism of Tislelizumab, an Investigational Anti-PD-1 Antibody, Is Differentiated from Pembrolizumab and Nivolumab. Proceedings of the 110th Annual Meeting of the American Association for Cancer Research; (Atlanta: AACR).

15. Lee, S.H., Lee, H.T., Lim, H., Kim, Y., Park, U.B., and Heo, Y.S. (2020). Crystal structure of PD-1 in complex with an antibody-drug tislelizumab used in tumor immune checkpoint therapy. Biochem. Biophys. Res. Commun. *527*, 226–231. https://doi.org/10.1016/j.bbrc.2020.04.121.

16. Ye, D., Liu, J., Zhou, A., Zou, Q., Li, H., Fu, C., Hu, H., Huang, J., Zhu, S., Jin, J., et al. (2021). Tislelizumab in Asian patients with previously treated locally advanced or metastatic urothelial carcinoma. Cancer Sci. *112*, 305–313. https://doi.org/10.1111/cas.14681.

17. Sandhu, S., Hill, A., Gan, H., Friedlander, M., Voskoboynik, M., Barlow, P., Townsend, A., Song, J., Zhang, Y., Liang, L., and Desai, J. (2018). Tislelizumab, an anti-PD-1 antibody, in patients with urothelial carcinoma (UC): results from an ongoing phase I/II study. Ann. Oncol. *29*, x28. https://doi.org/10.1093/annonc/mdy487.007.

18. Lee, A., and Keam, S.J. (2020). Tislelizumab: first approval. Drugs *80*, 617–624. https://doi.org/10.1007/s40265-020-01286-z.

19. Xu, J., Bai, Y., Xu, N., Li, E., Wang, B., Wang, J., Li, X., Wang, X., and Yuan, X. (2020). Tislelizumab plus chemotherapy as first-line treatment for advanced esophageal squamous cell carcinoma and gastric/gastroesophageal junction adenocarcinoma. Clin. Cancer Res. *26*, 4542–4550. https://doi.org/10.1158/1078-0432.Ccr-19-3561.

20. Lu, S., Wang, J., Yu, Y., Yu, X., Hu, Y., Ai, X., Ma, Z., Li, X., Zhuang, W., Liu, Y., et al. (2021). Tislelizumab plus chemotherapy as first-line treatment for locally advanced or metastatic nonsquamous NSCLC (RATIONALE 304): a randomized phase 3 trial. J. Thorac. Oncol. *16*, 1512–1522. https://doi.org/10.1016/j.jtho.2021.05.005.

21. Wang, J., Lu, S., Yu, X., Hu, Y., Sun, Y., Wang, Z., Zhao, J., Yu, Y., Hu, C., Yang, K., et al. (2021). Tislelizumab plus chemotherapy vs chemotherapy alone as first-line treatment for advanced squamous non-small-cell lung cancer: a phase 3 randomized clinical trial. JAMA Oncol. *7*, 709–717. https://doi.org/10.1001/jamaoncol.2021.0366.

22. Hoimes, C.J., Albany, C., Hoffman-Censits, J., Fleming, M.T., Trabulsi, E., Picus, J., Cary, C., Koch, M.O., Walling, R., Kelly, W., et al. (2018). A phase Ib/II study of neoadjuvant pembrolizumab (pembro) and chemotherapy for locally advanced urothelial cancer (UC). Ann. Oncol. *29*, viii726.

23. Cathomas, R., Petrausch, U., Hayoz, S., Schneider, M., Schardt, J.A., Seiler, R., Erdmann, A., Rothschild, S., Aeppli, S., Mach, N., et al. (2020). Perioperative chemoimmunotherapy with durvalumab (Durva) in combination with cisplatin/gemcitabine (Cis/Gem) for operable muscle-invasive urothelial carcinoma (MIUC): preplanned interim analysis of a single-arm phase II trial (SAKK 06/17). J. Clin. Oncol. *38*, 499. https://doi.org/10.1200/JCO.2020.38.6_suppl.499.

24. Martini, A., Jia, R., Ferket, B.S., Waingankar, N., Plimack, E.R., Crabb, S.J., Harshman, L.C., Yu, E.Y., Powles, T., Rosenberg, J.E., et al. (2019). Tumor downstaging as an intermediate endpoint to assess the activity of neoadjuvant systemic therapy in patients with muscle-invasive bladder cancer. Cancer *125*, 3155–3163. https://doi.org/10.1002/cncr.32169.

25. Mariathasan, S., Turley, S.J., Nickles, D., Castiglioni, A., Yuen, K., Wang, Y., Kadel, E.E., III, Koeppen, H., Astarita, J.L., Cubas, R., et al. (2018). TGFβ attenuates tumour response to PD-L1 blockade by contributing to exclusion of T cells. Nature *554*, 544–548. https://doi.org/10.1038/nature25501.

26. Wu, Y.M., Cieślik, M., Lonigro, R.J., Vats, P., Reimers, M.A., Cao, X., Ning, Y., Wang, L., Kunju, L.P., de Sarkar, N., et al. (2018). Inactivation of CDK12 delineates a distinct immunogenic class of advanced prostate cancer. Cell *173*, 1770–1782.e14. https://doi.org/10.1016/j.cell.2018.04.034.

27. Ragu, S., Matos-Rodrigues, G., and Lopez, B.S. (2020). Replication stress, DNA damage, inflammatory cytokines and innate immune response. Genes *11*, E409. https://doi.org/10.3390/genes11040409.

28. Long, Z.J., Wang, J.D., Xu, J.Q., Lei, X.X., and Liu, Q. (2022). cGAS/STING cross-talks with cell cycle and potentiates cancer immunotherapy. Mol. Ther. *30*, 1006–1017. https://doi.org/10.1016/j.ymthe.2022.01.044.

29. Elting, L.S., Cooksley, C., Bekele, B.N., Frumovitz, M., Avritscher, E.B.C., Sun, C., and Bodurka, D.C. (2006). Generalizability of cancer clinical trial results: prognostic differences between participants and nonparticipants. Cancer *106*, 2452–2458. https://doi.org/10.1002/cncr.21907.

30. Mailankody, S., and Prasad, V. (2017). Overall survival in cancer drug trials as a new surrogate end point for overall survival in the real world. JAMA Oncol. *3*, 889–890. https://doi.org/10.1001/jamaoncol.2016.5296.

31. Flaig, T.W., Tangen, C.M., Daneshmand, S., Alva, A., Lerner, S.P., Lucia, M.S., McConkey, D.J., Theodorescu, D., Goldkorn, A., Milowsky, M.I., et al. (2021). A randomized phase II study of coexpression extrapolation (COXEN) with neoadjuvant chemotherapy for bladder cancer (SWOG S1314; NCT02177695). Clin. Cancer Res. *27*, 2435–2441. https://doi.org/10.1158/1078-0432.Ccr-20-2409.

32. Bandini, M., Ross, J.S., Raggi, D., Gallina, A., Colecchia, M., Lucianò, R., Giannatempo, P., Farè, E., Pederzoli, F., Bianchi, M., et al. (2021). Predicting the pathologic complete response after neoadjuvant pembrolizumab in muscle-invasive bladder cancer. J. Natl. Cancer Inst. *113*, 48–53. https://doi.org/10.1093/jnci/djaa076.

33. Gupta, S., Sonpavde, G., Weight, C.J., McGregor, B.A., Gupta, S., Maughan, B.L., Wei, X.X., Gibb, E., Thyagarajan, B., Einstein, D.J., et al. (2020). Results from BLASST-1 (Bladder Cancer Signal Seeking Trial) of nivolumab, gemcitabine, and cisplatin in muscle invasive bladder cancer (MIBC) undergoing cystectomy. J. Clin. Oncol. *38*, 439. https://doi.org/10.1200/JCO.2020.38.6_suppl.439.

34. Pietrantonio, F., Lonardi, S., Corti, F., Infante, G., Elez, M.E., Fakih, M., Jayachandran, P., Shah, A.T., Salati, M., Fenocchio, E., et al. (2021). Nomogram to predict the outcomes of patients with microsatellite instability-high metastatic colorectal cancer receiving immune checkpoint inhibitors. J. Immunother. Cancer *9*, e003370. https://doi.org/10.1136/jitc-2021-003370.

35. Mezquita, L., Auclin, E., Ferrara, R., Charrier, M., Remon, J., Planchard, D., Ponce, S., Ares, L.P., Leroy, L., Audigier-Valette, C., et al. (2018). Association of the lung immune prognostic index with immune checkpoint inhibitor outcomes in patients with advanced non-small cell lung cancer. JAMA Oncol. *4*, 351–357. https://doi.org/10.1001/jamaoncol.2017.4771.

36. Pederzoli, F., Bandini, M., Raggi, D., Marandino, L., Basile, G., Alfano, M., Colombo, R., Salonia, A., Briganti, A., Gallina, A., et al. (2021). Is there a

detrimental effect of antibiotic therapy in patients with muscle-invasive bladder cancer treated with neoadjuvant pembrolizumab? Eur. Urol. *80*, 319–322. https://doi.org/10.1016/j.eururo.2021.05.018.

37. Salas-Benito, D., Pérez-Gracia, J.L., Ponz-Sarvisé, M., Rodriguez-Ruiz, M.E., Martínez-Forero, I., Castañón, E., López-Picazo, J.M., Sanmamed, M.F., and Melero, I. (2021). Paradigms on immunotherapy combinations with chemotherapy. Cancer Discov. *11*, 1353–1367. https://doi.org/10.1158/2159-8290.Cd-20-1312.

38. Xing, W., Zhao, L., Zheng, Y., Liu, B., Liu, X., Li, T., Zhang, Y., Ma, B., Yang, Y., Shang, Y., et al. (2021). The sequence of chemotherapy and toripalimab might influence the efficacy of neoadjuvant chemoimmunotherapy in locally advanced esophageal squamous cell cancer-a phase II study. Front. Immunol. *12*, 772450.

39. Hafeez, S., Horwich, A., Omar, O., Mohammed, K., Thompson, A., Kumar, P., Khoo, V., Van As, N., Eeles, R., Dearnaley, D., and Huddart, R. (2015). Selective organ preservation with neo-adjuvant chemotherapy for the treatment of muscle invasive transitional cell carcinoma of the bladder. Br. J. Cancer *112*, 1626–1635. https://doi.org/10.1038/bjc.2015.109.

40. Geynisman, D.M., Abbosh, P., Ross, E.A., Zibelman, M.R., Ghatalia, P., Anari, F., Ansel, K., Mark, J.R., Stamatakis, L., Hoffman-Censits, J.H., et al. (2021). A phase II trial of risk enabled therapy after initiating neoadjuvant chemotherapy for bladder cancer (RETAIN BLADDER): interim analysis. J. Clin. Oncol. *39*, 397. https://doi.org/10.1200/JCO.2021.39.6_suppl.397.

41. Galsky, M.D., Daneshmand, S., Chan, K.G., Dorff, T.B., Cetnar, J.P., O Neil, B., D'Souza, A., Mamtani, R., Kyriakopoulos, C., Garcia, P., et al. (2021). Phase 2 trial of gemcitabine, cisplatin, plus nivolumab with selective bladder sparing in patients with muscle- invasive bladder cancer (MIBC): HCRN GU 16-257. J. Clin. Oncol. *39*, 4503. https://doi.org/10.1200/JCO.2021.39.15_suppl.4503.

42. Carthon, B.C., Wolchok, J.D., Yuan, J., Kamat, A., Ng Tang, D.S., Sun, J., Ku, G., Troncoso, P., Logothetis, C.J., Allison, J.P., and Sharma, P. (2010). Preoperative CTLA-4 blockade: tolerability and immune monitoring in the setting of a presurgical clinical trial. Clin. Cancer Res. *16*, 2861–2871. https://doi.org/10.1158/1078-0432.Ccr-10-0569.

43. Rouanne, M., Bajorin, D.F., Hannan, R., Galsky, M.D., Williams, S.B., Necchi, A., Sharma, P., and Powles, T. (2020). Rationale and outcomes for neoadjuvant immunotherapy in urothelial carcinoma of the bladder. Eur. Urol. Oncol. *3*, 728–738. https://doi.org/10.1016/j.euo.2020.06.009.

44. Garcia del Muro, X., Valderrama, B.P., Medina, A., Cuellar, M.A., Etxaniz, O., Gironés Sarrió, R., Juan-Fita, M.J., Ferrer, F., Miras Rodríguez, I., Lendínez-Cano, G., et al. (2021). Phase II trial of durvalumab plus tremelimumab with concurrent radiotherapy (RT) in patients (pts) with localized muscle invasive bladder cancer (MIBC) treated with a selective bladder preservation approach: IMMUNOPRESERVE-SOGUG trial. J. Clin. Oncol. *39*, 4505. https://doi.org/10.1200/JCO.2021.39.15_suppl.4505.

45. Balar, A.V., Milowsky, M.I., O'Donnell, P.H., Alva, A.S., Kollmeier, M., Rose, T.L., Pitroda, S., Kaffenberger, S.D., Rosenberg, J.E., Francese, K., et al. (2021). Pembrolizumab (pembro) in combination with gemcitabine (Gem) and concurrent hypofractionated radiation therapy (RT) as bladder sparing treatment for muscle-invasive urothelial cancer of the bladder (MIBC): a multicenter phase 2 trial. J. Clin. Oncol. *39*, 4504. https://doi.org/10.1200/JCO.2021.39.15_suppl.4504.

46. Tenninge, S., Mogos, H., Eriksson, E., Netterling, H., Pelander, S., Johansson, M., Alamdari, F., Huge, Y., Aljabery, F., Svensson, J., et al. (2021). Control computerized tomography in neoadjuvant chemotherapy for muscle invasive urinary bladder cancer has no value for treatment decisions and low correlation with nodal status. Scand. J. Urol. *55*, 455–460. https://doi.org/10.1080/21681805.2021.1981996.

47. Mogos, H., Eriksson, E., Styrke, J., and Sherif, A. (2020). Computerized tomography before the final treatment cycle of neoadjuvant chemotherapy or induction chemotherapy in muscle-invasive urinary bladder cancer, cannot predict pathoanatomical outcomes and does not reflect prognosis-results of a single centre retrospective prognostic study. Transl. Androl. Urol. *9*, 1062–1072. https://doi.org/10.21037/tau-19-872.

48. Necchi, A., Bandini, M., Calareso, G., Raggi, D., Pederzoli, F., Farè, E., Colecchia, M., Marandino, L., Bianchi, M., Gallina, A., et al. (2020). Multiparametric magnetic resonance imaging as a noninvasive assessment of tumor response to neoadjuvant pembrolizumab in muscle-invasive bladder cancer: preliminary findings from the PURE-01 study. Eur. Urol. *77*, 636–643. https://doi.org/10.1016/j.eururo.2019.12.016.

49. Mountzios, G., Samantas, E., Senghas, K., Zervas, E., Krisam, J., Samitas, K., Bozorgmehr, F., Kuon, J., Agelaki, S., Baka, S., et al. (2021). Association of the advanced lung cancer inflammation index (ALI) with immune checkpoint inhibitor efficacy in patients with advanced non-small-cell lung cancer. ESMO open *6*, 100254. https://doi.org/10.1016/j.esmoop.2021.100254.

50. Corti, F., Lonardi, S., Intini, R., Salati, M., Fenocchio, E., Belli, C., Borelli, B., Brambilla, M., Prete, A.A., Quarà, V., et al. (2021). The Pan-Immune-Inflammation Value in Microsatellite Instability-High Metastatic Colorectal Cancer Patients Treated with Immune Checkpoint Inhibitors, *150* (European journal of cancer), pp. 155–167. https://doi.org/10.1016/j.ejca.2021.03.043.

51. Rebuzzi, S.E., Signori, A., Banna, G.L., Maruzzo, M., De Giorgi, U., Pedrazzoli, P., Sbrana, A., Zucali, P.A., Masini, C., Naglieri, E., et al. (2021). Inflammatory indices and clinical factors in metastatic renal cell carcinoma patients treated with nivolumab: the development of a novel prognostic score (Meet-URO 15 study). Ther. Adv. Med. Oncol. *13*, 17588359 211019642. https://doi.org/10.1177/17588359211019642.

52. Hu, J., Yu, A., Othmane, B., Qiu, D., Li, H., Li, C., Liu, P., Ren, W., Chen, M., Gong, G., et al. (2021). Siglec15 shapes a non-inflamed tumor microenvironment and predicts the molecular subtype in bladder cancer. Theranostics *11*, 3089–3108. https://doi.org/10.7150/thno.53649.

53. Baras, A.S., Gandhi, N., Munari, E., Faraj, S., Shultz, L., Marchionni, L., Schoenberg, M., Hahn, N., Hoque, M.O., Hoque, M., et al. (2015). Identification and validation of protein biomarkers of response to neoadjuvant platinum chemotherapy in muscle invasive urothelial carcinoma. PLoS One *10*, e0131245. https://doi.org/10.1371/journal.pone.0131245.

54. Hu, J., Othmane, B., Yu, A., Li, H., Cai, Z., Chen, X., Ren, W., Chen, J., and Zu, X. (2021). 5mC regulator-mediated molecular subtypes depict the hallmarks of the tumor microenvironment and guide precision medicine in bladder cancer. BMC Med. *19*, 289. https://doi.org/10.1186/s12916-021-02163-6.

STAR★METHODS

KEY RESOURCES TABLE

REAGENT or RESOURCE	SOURCE	IDENTIFIER
Chemicals, peptides, and recombinant proteins		
Cisplatin	Qilu Pharmaceutical, Shandong, China	http://en.qilu-pharma.com/
Gemcitabine	Hansoh Pharma, Jiangsu, China	http://www.hansoh.cn/en/
Tislelizumab	BeiGene, Beijing, China	https://www.beigene.com.cn/
TRIzol	Invitrogen, Carlsbad, CA, USA	NA
Chromium Next GEM Chip G Single Cell Kit	10× Genomics, Pleasanton, USA	48 rxns PN-1000120
Chromium Next GEM Single Cell 3' GEM, Library & Gel Bead Kit v3.1	10× Genomics, Pleasanton, USA	16 rxns PN-1000121
Chromium i7 Multiplex Kit	10× Genomics, Pleasanton, USA	96 rxns PN-120262
Deposited data		
Raw single cell RNA-seq data	This paper	GSA: HRA003068
Raw bulk RNA-seq data	This paper	GSA: HRA003074
Software and algorithms		
R software	https://www.r-project.org/	Version: 4.0.5
Other		
RNA sequencing platform	BGISEQ-500 platform, Shenzhen, China	NA
Illumina NovaSeq 6000 System	Illumina, San Diego, USA	NA
Agilent 2100 bioanalyzer	Thermo Fisher Scientific, MA, USA	NA
NanoDrop	Thermo Fisher Scientific, MA, USA	NA
Chromium Single Cell Controller instrument	10× Genomics, Pleasanton, CA, USA	NA

RESOURCE AVAILABILITY

Lead contact

Further information and requests for resources and data should be directed to and will be fulfilled by the lead contact, Xiongbing Zu, PhD (zuxbxy@csu.edu.cn).

Materials availability

This study did not generate new unique reagents.

Data and code availability

Single-cell RNA-seq data (GSA: HRA003068) and bulk RNA-seq data (GSA: HRA003074) reported in this paper have been deposited in the Genome Sequence Archive in National Genomics Data Center, China National Center for Bioinformation, Chinese Academy of Sciences that are publicly accessible at https://ngdc.cncb.ac.cn/gsa.

This paper does not report original code.

Any additional information required to reanalyze the data reported in this paper is available from the lead contact upon request.

EXPERIMENTAL MODEL AND SUBJECT DETAILS

Ethics statement

This study was approved by the Ethics Committees of all centers (ethical number: 202,112,241). The authors are accountable for all aspects of the work in ensuring that questions related to the accuracy or integrity of any part of the work are appropriately investigated and resolved. Written informed consents were obtained from participants or their immediate families.

Human subjects

Chinese adults, both male and female, with histologically confirmed MIBC, receiving at least two cycles of standardized neoadjuvant treatment and subsequent surgery, were enrolled in the study. Demographic information (i.e., age and gender) was reported in Table 1.

CellPress
OPEN ACCESS

METHOD DETAILS

Study design, outcomes and patient selection

This is a multi-center real-world retrospective cohort study evaluating the efficacy and safety of NAC, NICB, and NAC.NICB in patients with MIBC. The first research outcome was pathologic downstaging, including complete pathological response (CR: pT0N0M0) and partial response (PR: pTis, Ta, T1 N0M0). pT2-4N0M0 with an enlarged tumor volume, pN+ and pM+ were defined as progression diseases (PD), and the remaining status were defined as stable diseases (SD). The secondary outcome was the recurrence status for patients who received bladder preservation treatment.

Inclusion criteria: 1) patients with confirmed MIBC; 2) patients receiving at least two cycles of standardized neoadjuvant treatment; 3) patients receiving RC, maximal transurethral resection of the bladder tumor (TURBT) or partial cystectomy after neoadjuvant treatment for precise pathologic staging. Exclusion criteria: 1) patients were pathologically diagnosed as other metastatic cancers instead of MIBC; 2) patients receiving complete TURBT before neoadjuvant treatment, because the complete pre-TURBT might influence the efficacy evaluation of neoadjuvant treatments.

Neoadjuvant treatment schedules

NICB: Tislelizumab 200 mg administered intravenously (IV) Q3W.

NAC: Cisplatin (70 mg/m^2) IV on day 1, gemcitabine (1000 mg/m^2) on day 1 and day 8, Q3W.

NAC.NICB: Based on the neoadjuvant treatments sequence, this schedule included three subgroups. NAC-before-NICB: Cisplatin (70 mg/m^2) IV on day 1, Tislelizumab 200mg on day 2, gemcitabine (1000 mg/m^2) on day 1 and day 8, Q3W; NICB-before-NAC: Tislelizumab 200mg on day 1, cisplatin (70 mg/m^2) IV on day 2, gemcitabine (1000 mg/m^2) on day 2 and day 8, Q3W; NICB-concur-NAC: Tislelizumab 200 mg IV on day 1, cisplatin (70 mg/m^2) IV on day 1, gemcitabine (1000 mg/m^2) on day 1 and day 8, Q3W.

Clinicopathological characteristics collection and definition

We collected the clinical characteristics recorded at the initiation of neoadjuvant treatments. Treatment related adverse events (TRAE) were assessed per National Cancer Institute Common Terminology Criteria for Adverse Events v4.03. Concomitant antibiotic therapy was defined as any antibiotics administration within one month before the first neoadjuvant treatment dose or during treatments. All hematologic parameters were assessed within one day before the first neoadjuvant treatment dose. Then, we defined several comprehensive indexes with potential predicting value for immunotherapy response, such as neutrophil-to-lymphocyte ratio (NLR) and platelet-to-lymphocyte ratio (PLR).[35,49–51] All pathologic sections from fifteen centers were centrally reviewed by two independent pathologists. Pathological characteristics included the grade and histology of TURBT biopsy samples before neoadjuvant treatment, in addition to the postoperative pathological stage.

Biomarker analysis

Four response samples and six resistance samples from NAC.NICB cohort were collected before treatments and were immediately stored in liquid nitrogen. Total RNA of these samples was extracted using TRIzol (Invitrogen, Carlsbad, CA, USA). Subsequently, NanoDrop and Agilent 2100 bioanalyzer (Thermo Fisher Scientific, MA, USA) were used to quantify total RNA. Then, we constructed the mRNA library. All of the total RNA were purified and fragmented into small pieces. Then, first-strand cDNA and second-strand cDNA were synthesized. After incubating with A-tailing mix and RNA Adapter Index for end repair, the cDNA fragments were further amplified by using PCR. We constructed the final library (single-stranded circular DNA) based on the qualified double-stranded PCR products. Finally, we performed RNA sequencing (BGISEQ-500 platform, Shenzhen, China) on these samples, and calculated the gene expression levels by using RSEM (v1.2.12). Then, we filtered differentially expressed genes (DE-Gs) between these two groups using the ''DESeq2'' R package with criteria of adjusted $p < 0.05$ and $|\log \text{fold change (FC)}| > 1.5$. GO and KEGG analysis were performed based on these DE-Gs using the ''Clusterprofile'' R package. We collected 19 ICB efficacy related signatures, 2 NAC efficacy related signatures, and four stroma signatures from previous studies and summarized them in Table S7.[25,52,53] We then calculated the enrichment scores of these pathways using the ssGSEA algorithm.

We performed single cell RNA sequencing (OE Biotech Co, Ltd, Shanghai, China) on two response samples and one resistance sample from NICB cohort. The detailed sequencing procedures, data preprocessing, and analysis methods have been reported in our previous study.[54] Briefly, the tumor samples were prepared into single-cell suspension, which was subsequently loaded on a Chromium Single Cell Controller instrument (10× Genomics, Pleasanton, CA, USA) to generate the single-cell gel beads in emulsions. The Cell Ranger (version 2.2.0) was used to process the raw data. demultiplex cellular barcodes, map reads to the transcriptome, and down-sample reads. Then, a raw unique molecular identifier (UMI) count matrix was produced. The raw count matrixes were used to create Seurat object using ''Seurat'' R package and the inclusion criteria for high quality cells were set as: numbers of unique molecular identifier (UMI) more than 1000, genes more than 200, log10GenesPerUMI more than 0.70 and mitochondrial percent less than 20%. After quality control, we performed principal component analysis (PCA) on all single cells and identified cells clusters by using FindClusters function. Conventional markers described in our previous study were used to categorize cells into a known biological cell type.[54] We applied the InferCNV package to detect the CNVs of all cells and confirmed the epithelial cells as the malignant bladder cancer cells.[54] The Seurat Findallmarker function was used to identify preferentially expressed genes in each

cluster. GSEA analysis was performed based on the preferentially expressed genes of each cluster. As for bladder cancer cell clusters, we explored their functions by using the ''Clusterprofile'' R package. Then, we annotated bladder cancer cell clusters according to their most significant functions.

QUANTIFICATION AND STATISTICAL ANALYSIS

For categorical variables, comparisons between patient subgroups were performed by using the chi-square test or Fisher exact test. For comparisons of continuous variables fitting normal distribution, we conducted a t-test or one-way ANOVA analysis; otherwise, the Mann-Whitney U or Kruskal-Wallis H test was conducted. Especially for NAC.NICB cohort, we developed and validated a clinical nomogram to calculate treatment response score using the ''rms'' R package. Receiver operating characteristic (ROC) curves were plotted using the ''pROC'' R package. We compared the AUCs by using de-Long test. Decision curve analysis (DCA) was performed using the ''dca'' R package. All data visualization and statistical analyses were performed in R software (Version: 4.0.5). Analyses with two-sided $p < 0.05$ were considered statistically significant.